Temperature-dependent magnetization reversal in (Co/Pt)/Ru multilayers

Joseph E. Davies,[1,2] Olav Hellwig,[3] Eric E. Fullerton,[3,4] and Kai Liu[1,*]
[1]*Physics Department, University of California, Davis, California 95616, USA*
[2]*National Institute of Standards and Technology, Gaithersburg, Maryland 20899, USA*
[3]*Hitachi Global Storage Technologies, San Jose, California 95135, USA*
[4]*Center for Magnetic Recording Research, University of California-San Diego, La Jolla, California 92093-0401, USA*
(Received 29 October 2007; published 16 January 2008)

Antiferromagnetically coupled (Co/Pt)/Ru multilayers with perpendicular anisotropy have been shown to exhibit both vertically and laterally correlated magnetization reversal modes. In this work, the magnetization reversal of a multilayer film whose layer thicknesses have been tuned to be at the phase boundary between the two reversal modes has been investigated as a function of temperature, using the first-order reversal curve (FORC) method. At high temperatures, reversal via vertically correlated stripe domains throughout the film thickness is observed, similar to that in Co/Pt films without the Ru spacers. At low temperatures, antiferromagnetic (AF) interlayer exchange coupling dominates, and laterally correlated reversal is observed with an AF coupled remanent state. Under magnetic field cycling, dipolar fields can transform the sample back into a vertically correlated domain state, thus leading to an exotic behavior with FORC's existing outside the major hysteresis loop. Calculations show that the laterally correlated reversal mode is indeed slightly more stable, and the crossover to vertically correlated reversal can be induced by temperature as well as magnetic field.

DOI: 10.1103/PhysRevB.77.014421 PACS number(s): 75.60.−d, 75.70.Kw, 75.30.Kz, 75.70.Cn

I. INTRODUCTION

Magnetic thin films with strong perpendicular anisotropy, e.g., Co/Pt and Co/Pd multilayers, have been a topic of increasing interest due to their easily tunable magnetic properties and possible applications in perpendicular magnetic recording and patterned media.[1–15] The magnetization reversal process in these systems usually involves the formation of vertically correlated stripe domains, through the entire multilayer film stack resulting from a competition between ferromagnetic (FM) exchange, anisotropy, and dipolar energies.[1] The energy balance can be further tailored through the addition of Ru spacer layers with appropriate thicknesses, which establishes antiferromagnetic (AF) interlayer exchange coupling.[15–18] In $[(\mathrm{Co/Pt})_{X-1}/\mathrm{Co/Ru}]_N$ multilayers, both vertically and laterally correlated domain states have been observed.[6,18–20] The reversal modes are determined largely by the sample thickness and magnetization and by the strength of the AF interlayer coupling. In these samples, the competition between reversal modes is tuned by N, the number of Co/Pt stacks separated by Ru spacer layers, and X, the number of Co layers per Co/Pt stack (Fig. 1, inset). For thick samples with relatively weak AF coupling (or fewer number of Ru spacers), the vertically correlated mode is energetically favored. Strong dipolar fields overcome the AF interlayer exchange coupling, leading to up and down stripe domains through the film thickness. For thinner samples with strong AF coupling, a laterally correlated mode is favored. The interlayer AF exchange coupling dominates, leading to antiparallel alignment between adjacent FM stacks. The remanent state energies for the two modes and a corresponding phase diagram at room temperature have previously been calculated, in good agreement with major loop and magnetic imaging measurements.[19,20] Of particular interest are samples along the phase boundary, expected to display a delicate balance among magnetostatic, domain wall, and interlayer exchange energies. Coexistence of the reversal modes has indeed been shown by magnetic imaging of the AF domains in the laterally correlated samples where the domain boundaries consist of alternating vertically correlated FM domains.[20] In such samples, it should be possible to alter the magnetic correlations from vertical to horizontal and vice versa via temperature variation or magnetic field cycling.[20–22] However, experimentally such complex behaviors are more challenging to characterize and interpret.

In this work, we have investigated temperature dependent magnetization reversal modes in $[(\mathrm{Co/Pt})_{X-1}/\mathrm{Co/Ru}]_N$ samples. The reversal behavior was investigated using a

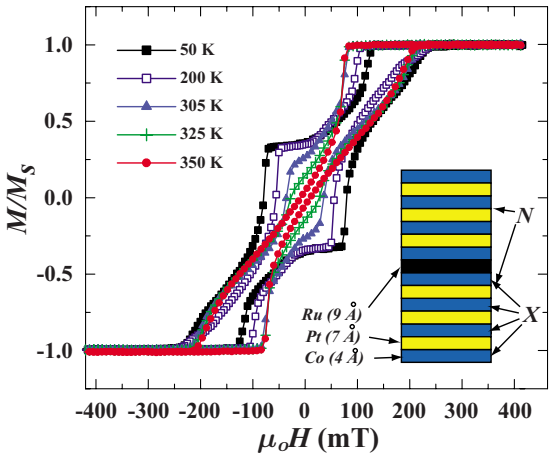

FIG. 1. (Color online) Major hysteresis loops for a $[(\mathrm{Co/Pt})_{X-1}/\mathrm{Co/Ru}]_N$ film with $N=3$ and $X=10$ at different temperatures, showing the gradual transition from fully vertically correlated reversal at 350 K to laterally correlated reversal at lower temperatures. The inset shows a schematic of the multilayer structure, where X corresponds to the number of Co layers in each Co/Pt stack, while N represents the number of Co/Pt stacks.

first-order reversal curve (FORC) method.[7,23–25] FORC has been utilized previously to "fingerprint" the reversal behavior of Co/Pt multilayers, without Ru spacer layers.[7] The current FORC analysis of the $[(Co/Pt)_{X-1}/Co/Ru]_N$ samples allows the identification of the laterally and vertically correlated reversal modes as well as the complex interplay between them as temperature and magnetic field are varied. In particular, a unique and rather exotic behavior is observed, with FORC's partially extruding outside of the major loop. The magnetic energies associated with these modes are investigated, revealing a delicate balance between the two reversal modes.

II. EXPERIMENTAL DETAILS

Samples under investigation are $\{[Co(4\ Å)/Pt(7\ Å)]_{X-1}/Co(4\ Å)/Ru(9\ Å)\}_N$ multilayers. Specifically considered here is a film with $N=3$ and $X=10$, which is at the phase boundary between laterally and vertically correlated reversal modes.[18] For comparison, a $(Co/Pt)_{30}$ multilayer film with 30 bilayer repeats and another film with $N=3$ and $X=5$ are also investigated. The $(Co/Pt)_{30}$ multilayer film displays only vertically correlated reversal, whereas the $N=3$ and $X=5$ film is strongly AF coupled and displays laterally correlated reversal only. The samples were grown by magnetron sputtering at 0.4 Pa (3 mtorr) Ar pressure and ambient temperature. We used Si substrates coated with Si_3N_x and a 200 Å Pt buffer layer. The Co and Pt layer thicknesses were chosen to obtain perpendicular anisotropy,[26] while the Ru thickness was used to maximize the AF-interlayer coupling between adjacent Co/Pt stacks.[18]

Magnetic properties were studied using an alternating gradient magnetometer and vibrating sample magnetometer. The temperature was controlled by a continuous-flow liquid helium cryostat as well as a high temperature furnace. In order to study the magnetization reversal behavior, we have employed a FORC technique, as described in prior publications.[7,25,27] After saturation, the magnetization M is measured starting from a reversal field H_R back to positive saturation, tracing out a FORC. A family of FORC's is measured at different H_R, with equal field spacing, covering the entire major loop from the onset of reversal until true saturation. A FORC distribution is determined by a mixed second order derivative of the magnetization $M(H_R,H)$,[23,24] $\rho(H_R,H) \equiv -(1/2)[\partial^2 M(H_R,H)/\partial H_R \partial H]$. This derivative eliminates the purely reversible components of the magnetization.[28,29] Thus, any nonzero ρ corresponds to *irreversible* switching processes. A plot of the distribution ρ versus H and H_R, such as a two-dimensional contour plot, can then reveal the details of the magnetization reversal. For each curve with a specific reversal field H_R, the magnetization M is measured with increasing applied field H; the corresponding FORC distribution ρ is represented by a horizontal line scan at that H_R along H in the FORC diagram [e.g., Figs. 2(a) and 2(c)]. As shown recently, the FORC technique is very sensitive to irreversible switching processes,[7,25] distributions of magnetic characteristics,[30] and powerful in qualitative and quantitative magnetic phase identification.[27,31] It is ideally suited for "fingerprinting" the presence of magnetic inhomogeneities, which are manifested as unique patterns in FORC diagrams.

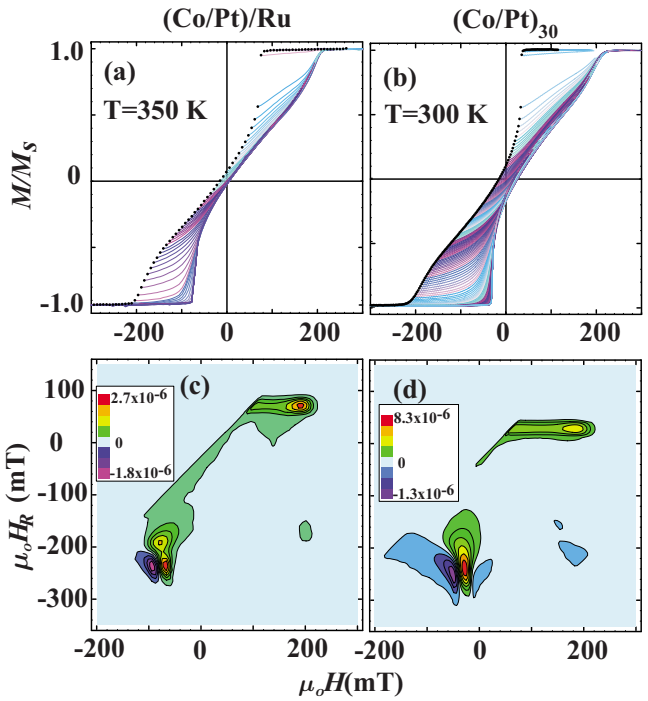

FIG. 2. (Color online) FORC's (top) and respective FORC distribution (bottom) at 350 K for the [(a) and (c)] (Co/Pt)/Ru, $N=3$ and $X=10$, sample compared to those of a [(b) and (d)] $[Co(4\ Å)/Pt(7\ Å)]_{30}$ multilayer film at 300 K.

III. RESULTS

A. Major hysteresis loops

Major hysteresis loops have been measured at different temperatures (Fig. 1). At 350 K, starting from positive saturation, the loop shows an abrupt reversal onset at $\mu_o H = 80$ mT and reaches apparent negative saturation at −220 mT. The remanent magnetization M_r is only 7% of the saturation magnetization M_S. This loop shape is typical of a vertically correlated reversal mode via stripe domains. As temperature is lowered, a second abrupt reversal step progressively emerges within the major loop. The first reversal field gradually shifts to more positive fields, while the second reversal field, along with the negative saturation field, shifts oppositely to more negative fields. At 50 K, the two-stage reversal is clearly established, with the step formed at a magnetization level of about 33% of M_S, indicating a separate center stack reversal. The appearance of the step is characteristic for a stack-by-stack reversal with a laterally uniform state at remanence. Because the sample has an odd number of layers ($N=3$), there will be a finite remanent magnetization when the sample is in an AF state. The remanent magnetization will be $1/N$ (or 33% for $N=3$) of the saturation magnetization. However, during reversal portions of the major loop are still reminiscent of vertically correlated reversal. In order to obtain a better understanding of the magne-

tization reversal details, FORC measurements have been taken.

B. Vertically correlated reversal

A family of FORC's for the $\{[Co(4Å)/Pt(7Å)]_9/Co(4\ Å)/Ru(9\ Å)\}_3$ sample at 350 K is shown in Fig. 2(a), where the black dots represent the starting points of the FORC's. The corresponding FORC distribution is shown in Fig. 2(c). For comparison, shown in Figs. 2(b) and 2(d) are those of a $[Co(4\ Å)/Pt(7\ Å)]_{30}$ multilayer measured at 300 K, which has a similar layer structure but without the Ru spacers. Remarkable similarities are observed between the families of FORC's, the major hysteresis loops (delineated by the outer boundaries of FORC's), and the FORC distributions for the two samples. In our previous study of $(Co/Pt)_X$ multilayers with perpendicular anisotropy ($X \geqslant 10$), we have found that the reverse domains are vertically correlated throughout the film thickness. In progressing from positive to negative saturation, there are three stages of reversal with distinct features in both the major loop and the FORC diagram (plotted in H-H_R coordinates):[7] an initial rapid and irreversible domain propagation from already nucleated sites that leads to a precipitous drop in the magnetization and a horizontal ridge in the FORC diagram; a subsequent mostly reversible process of domain width expansion-contraction with little change in the domain morphology, which corresponds to gradual changes in magnetization and a shallow plateau in the FORC diagram with $\rho \sim 0$; and finally an irreversible domain annihilation process, when reaching negative saturation, thus yielding a vertical negative-positive pair of peaks in the FORC diagram. This set of FORC patterns is characteristic of the vertically correlated magnetization reversal in Co/Pt multilayers. Furthermore, the size of the shallow plateau (i.e., the field spacing along H_R between the horizontal ridge and the negative-positive pair) increases with the number of multilayer repeats X. For example, a $(Co/Pt)_X$ sample with $X=10$ has a measured planar region extending ~60 mT, whereas a $X=30$ sample has a region of ~200 mT [Fig. 2(d)], comparable to that in the present $[(Co/Pt)_9/Co/Ru]_3$ sample [Fig. 2(c)]. The FORC's and FORC diagrams in Fig. 2 therefore confirm that at 350 K, magnetization reversal in $[(Co/Pt)_9/Co/Ru]_3$ proceeds via vertically correlated domains throughout the sample.

C. Laterally correlated reversal

As the temperature is decreased from 350 to 200 K, a second abrupt reversal step emerges, indicating the preference of a laterally correlated stack-by-stack reversal due to a lower energy of the AF coupled remanent state. FORC's taken at 200 K are shown in Fig. 3(a). Strikingly, a majority of the FORC's reveal some portions that exist outside of the major loop (shown more explicitly in Figs. 4 and 5). The corresponding FORC distribution [Fig. 3(c)] is much more complex than that at 350 K [Fig. 2(c)].

For comparison, the reversal behavior of a strongly AF coupled three stack structure,[18] a $[(Co/Pt)_4/Co/Ru]_3$ sample, is shown in Figs. 3(b) and 3(d). For that sample, there are

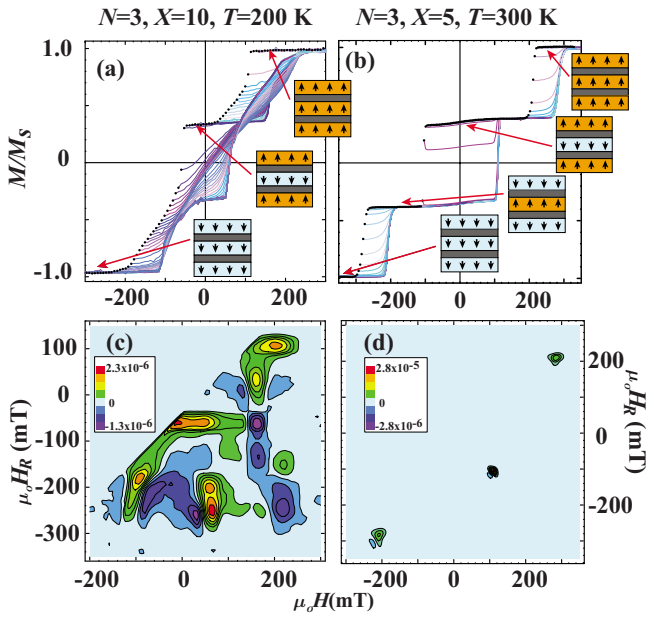

FIG. 3. (Color online) FORC's (top) and FORC distributions (bottom) for the [(a) and (c)] $N=3$ and $X=10$ sample at 200 K, compared to a [(b) and (d)] $N=3$ and $X=5$ sample at 300 K. The inset schematics show stack-by-stack reversal for both samples. In the $N=3$ and $X=5$ sample, the AF coupling is strong enough to trigger a *stack inversion*. (d) The three abrupt reversal steps result in sharp peaks in the FORC distribution. The $N=3$ and $X=10$ sample exhibits only two reversal steps, indicating that the AF coupling is not strong enough to drive the system through a stack inversion.

three step-like abrupt magnetization drops in the major loop [Fig. 3(b)]. The first step corresponds to the reversal of the center Co/Pt stack, as resolved by depth sensitive Kerr measurements.[32] Due to the small number of repeats ($X=5$), dipolar fields are not strong enough to trigger vertically synchronized stripe domain formation throughout all three stacks of the film. At the second reversal step, the entire magnetic configuration inverts, i.e., the two outer Co/Pt stacks switch to negative saturation while the center stack switches back to positive saturation due to the strong AF interlayer exchange coupling. Finally, at the last reversal step, the center stack reverses once more to bring the sample to negative saturation. These three reversal steps are manifested as three localized peaks in the FORC diagram at $\mu_o H_R \sim 200$, −100, and −300 mT, respectively [Fig. 3(d)].

The reversal behavior of the $[(Co/Pt)_9/Co/Ru]_3$ sample distinctly differs from that of the $[(Co/Pt)_4/Co/Ru]_3$ sample. In order to better understand this more complex reversal behavior, it is helpful to isolate the FORC's for different ranges of $\mu_0 H_R$ starting from positive saturation. Key stages of the reversal are shown in Fig. 4 for different reversal fields $\mu_0 H_R$. In panels (a), (c), and (e), the major loop is sketched by black dots along the decreasing-field branch and a solid black line along the increasing-field branch. Corresponding schematics of the reversal processes are shown in Fig. 5.

The first stage of reversal is represented by a group of FORC's with $\mu_0 H_R > -30$ mT [Fig. 4(a)]. The outer boundary of this group of FORC's delineates a minor loop, whose

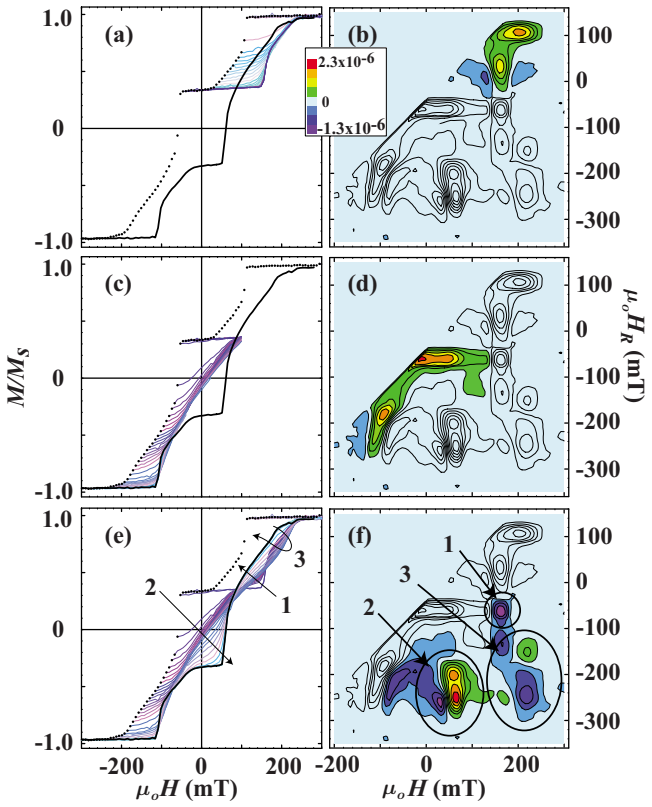

FIG. 4. (Color online) Partial sets of FORC's (left) and corresponding shaded portions of the FORC distribution (right) for the $N=3$ and $X=10$ sample at 200 K. At $\mu_0 H_R > -30$ mT, the reversal of the middle Co/Pt stack is shown in (a) and (b). At $\mu_0 H_R < -30$ mT, the initial reversal of the two outer Co/Pt stacks is shown in (c) and (d); the continuation of the reversal at higher applied fields is shown in (e) and (f), where the film returns to a vertically correlated FM stripe domain structure, resulting in additional features in the (f) FORC distribution. Arrows 1–3 in (e) correspond to the moving directions of successive FORC's, which lead to features 1–3 in the (f) FORC distribution.

magnetization is 1/3 of the total magnetization. Note that this group of FORC's resembles the reversal of a $(Co/Pt)_{10}$ multilayer and has extruded outside of the major loop. The FORC distribution for this range of $\mu_0 H_R$ [Fig. 4(b), shaded region] exhibits a horizontal ridge followed by a negative-positive region with a separation of ~60 mT in $\mu_0 H_R$, again consistent with a single $(Co/Pt)_{10}$ multilayer reversal. These characteristics indicate that a single Co/Pt stack within the $[(Co/Pt)_9/Co/Ru]_3$ multilayer has reversed at remanence. Since the center stack is AF coupled at both interfaces, it has twice the interlayer exchange energy and thus reverses first [Figs. 5(a) and 5(b)], as was also confirmed by depth sensitive Kerr measurements.[32]

The second stage of the reversal is represented by a group of FORC's with $\mu_0 H_R < -30$ mT, i.e., beyond the apparent step in the major loop [Fig. 4(c)]. The FORC distribution has several sets of features. The first feature [Fig. 4(d), highlighted region] shows once more the characteristic horizontal ridge at $\mu_0 H_R = -60$ mT, followed by a larger planar region and finally a negative-positive pair, which are characteristics

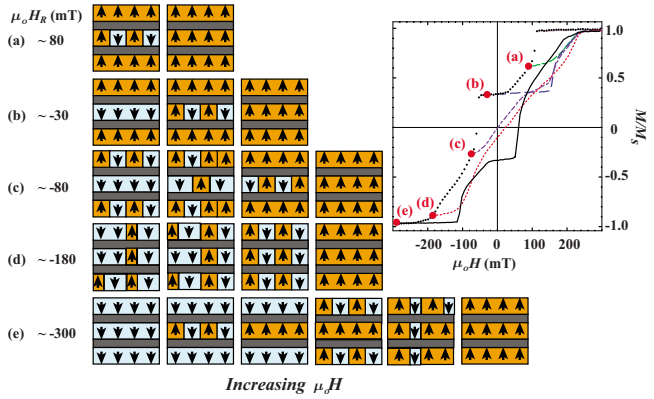

FIG. 5. (Color online) Illustration of the different reversal modes and domain states encountered for the $N=3$ and $X=10$ sample at 200 K along five representative FORC's, as highlighted in the inset. The increasing-field branch of the major magnetic hysteresis loop is sketched by (e) and the solid line in the inset. The applied field is perpendicular to the Co/Pt stacks.

for perpendicularly correlated stripe domain nucleation, propagation, and annihilation. Here, the planar region spans ~120 mT in $\mu_0 H_R$, consistent with the reversal of a Co/Pt multilayer with 20 repeats. Since the middle Co/Pt stack has already reversed, this pattern indicates a *synchronized* nucleation and reversal onset of the outer two Co/Pt stacks. This is different from the steplike inversion of the magnetic structure as seen in the $[(Co/Pt)_4/Co/Ru]_3$ sample [Fig. 3(d)].

There are additional features as the outer two Co/Pt stacks continue to reverse. Part of the center stack reverses back to the original magnetization direction to form vertically correlated FM stripe domains and thus triggers a transition in the reversal behavior during the external field sweep itself. The FORC's starting at $-80 \text{ mT} < \mu_0 H_R < -50$ mT continue to extend outside of the major loop at $\mu_0 H > 100$ mT, but deviate from those originated at $\mu_0 H_R > -30$ mT. In the field range of $140 \text{ mT} < \mu_0 H < 170$ mT, the FORC's actually cross over and move back toward the major loop, as indicated by arrow 1 in Fig. 4(e), showing the decay of the reversal step established by the FORC's in Fig. 4(a). This leads to a localized negative valley in the FORC distribution, as highlighted by circle 1 in Fig. 4(f). The FORC's starting at $\mu_0 H_R < -170$ mT exhibit more exotic behaviors. In the range of $0 < \mu_0 H < 100$ mT, the FORC's develop a sharp corner [indicated by arrow 2 in Fig. 4(e)], conforming to that in the major loop. This leads to a negative-positive pair of features in the FORC distribution highlighted by circle 2 in Fig. 4(f). In the field range of $\mu_0 H > 150$ mT, the FORC's continue the aforementioned crossover and subsequently fall back onto the major loop, as indicated by arrow 3 in Fig. 4(e). This leads to another negative FORC feature indicated by circle 3 in Fig. 4(f).

D. Crossover between laterally and vertically correlated reversal

The complex reversal behavior manifested in the FORC diagram confirms the delicate balance between laterally and

vertically correlated reversals. A transition between the two states can be tuned by temperature or magnetic field cycling. To better illustrate the latter, domain configurations along five representative FORC's at 200 K are schematically shown in Fig. 5. The first two FORC's [(a) and (b)] correspond to the initial switching of the center Co/Pt stack only. The reversal within the center stack is vertically correlated, while the outer two stacks remain laterally correlated in a positively saturated state. Immediately following the precipitous drop in magnetization at the second reversal step, for the FORC reversing at $\mu_0 H_R = -80$ mT [Fig. 5, row (c)], the middle Co/Pt stack is reversed completely with the outer two stacks nucleating initial reverse domains. With increasing field $\mu_0 H$, a mixture of vertically and laterally correlated reverse domains forms. Dipolar fields from the reverse domains in the outer two stacks help to renucleate reverse domains in the center stack, thus triggering formation of vertically correlated FM stripe domains. A residual laterally correlated portion of the reversal is indicated by the still observable kink around $\mu_0 H = 170$ mT [Fig. 5, inset (c)]. At more negative reversal fields, e.g., $\mu_0 H_R = -180$ mT, as shown in Fig. 5, row (d), the FORC's closely resemble those in the high temperature regime, indicating the increasing dominance of vertically correlated reversal. When performing symmetric minor loops with maximum applied fields of ±100–±250 mT, we obtain a continuous loop shape characteristic of vertically correlated FM stripe domain reversal (see Fig. 29 in Ref. 32). Only when finally the external field is increased well beyond ±300 mT [Fig. 5, row (e)], thus annihilating all remaining FM bubble domains,[7] does the reversal mode change back to the major loop: the middle Co/Pt stack reverses first, followed by reversal of the outer two stacks; there are also partial renucleation events in the middle stack due to dipolar fields produced by the domains in the outer stacks.

The change in reversal mode from a stack-by-stack reversal to vertically correlated FM domains can be explained in terms of the magnetic energy. We can compare the energy difference between the laterally correlated (AF coupled) and vertically correlated (FM domain) remanent states.[6,19] For each remanent configuration, the total energy can be expressed as the sum of the magnetostatic demagnetization, domain wall, and interlayer exchange energies,

$$E = E_{demag} + E_{wall} + E_{exchange}. \tag{1}$$

For the vertically correlated remanent state, the corresponding terms are[32]

$$E_{FM} = \frac{16 M_S^2 D}{\pi^2} \sum_n^{odd} \frac{1}{n^3} [1 - \exp(-n\pi t/D)] + \frac{4\sqrt{AK_U}t}{D} + (N-1)J_{AF}, \tag{2}$$

where $M_s = 7 \times 10^5$ A/m is the saturation magnetization, $D \sim 900$ Å is the domain width, $t = 327$ Å is the total film thickness, $A \sim 10^{-11}$ J/m is the exchange stiffness, $K_u = 5 \times 10^5$ J/m^3 is the uniaxial perpendicular anisotropy constant, and $J_{AF} = 0.46$ mJ/m^2 is the exchange energy density per Ru layer.[32] For the laterally correlated AF coupled state,

$$E_{AF} = N 2\pi M_S^2 t' - 2J_{AF}, \tag{3}$$

where t' is the film thickness of each Co/Pt stack and the domain wall energy is zero.

These estimates show that the laterally correlated AF coupled state is slightly more stable at remanence than the vertically correlated FM domain state by 0.8 mJ/m^2. Note that in Co/Pt multilayers, without Ru spacers, the FM domain state is always more stable. It is the introduction of the AF interlayer coupling mediated by the Ru that has increased E_{FM} and lowered E_{AF} each by $2J_{AF}$, or a total difference of $4J_{AF} = 1.8$ mJ/m^2 at 300 K. The J_{AF} value is experimentally determined from the exchange field H_E in the aforementioned $[(Co/Pt)_4/Co/Ru]_3$ sample, which displays a purely AF coupled laterally correlated reversal mode,[18]

$$2J_{AF} = H_E M_S t'. \tag{4}$$

This accounts for the two Ru spacers present in the sample. As shown in Fig. 6(a), with increasing temperature, J_{AF} decreases from 0.8 mJ/m^2 at 35 K to 0.3 mJ/m^2 at 400 K. In comparison, the temperature dependence of M_S is relatively weaker in this range, showing a 15% decrease from

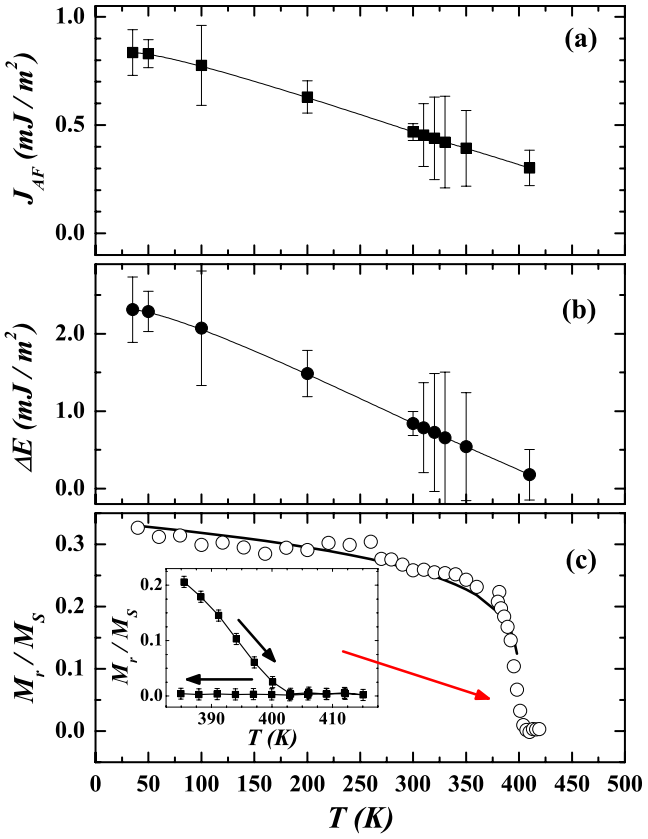

FIG. 6. (Color online) Temperature dependence of (a) the interfacial AF exchange coupling J_{AF}, (b) the energy difference $\Delta E = E_{FM} - E_{AF}$ considering only the temperature dependence of J_{AF}, and (c) the normalized remanent magnetization for the AF coupled state established at 40 K. The inset in (c) shows the direction of temperature cycling near 400 K. Solid lines are guides to the eye.

35 to 400 K; since the energy difference $\Delta E = E_{FM} - E_{AF}$ scales with $\sqrt{K_U}$, the temperature dependence of K_U is less critical; it is the temperature dependence of J_{AF} that has a dominant effect on ΔE. For simplicity, considering only the J_{AF} temperature dependence, the calculated ΔE also decreases rapidly with temperature, vanishing at ~440 K, as shown in Fig. 6(b). This simplified estimate suggests that the vertically correlated remanent domain state becomes stable above 440 K.

To test the thermal stability of the laterally correlated state, we have studied the temperature dependence of the remanent magnetization M_r. The laterally correlated state was first established at $T=40$ K by the following field cycling: applying a field $\mu_0 H$ of 500 mT perpendicular to the film to saturate the sample, then reducing the field to −50 mT to ensure the middle layer has reversed completely [similar to Fig. 3(a)] and finally setting the field to zero and achieving $M_r/M_S = 1/3$. The remanent magnetization was then measured as a function of temperature from 40 to 420 K [Fig. 6(c)] and then returning to 40 K. Major hysteresis loops were also measured before and after the measurement to ensure the high temperatures did not cause any significant change to the multilayer structure.

The measurement shows a gradual decrease of M_r with increasing temperature over 50–350 K, before it abruptly vanishes around 400 K [Fig. 6(c), inset], which is in quite good agreement with our simplified estimate. The small remanent magnetization is a signature of the vertically correlated stripe domain state. As temperature is reduced back to 40 K, the magnetization remains at zero, showing that the conversion of the AF coupled state to the FM stripe domains is irreversible. In accordance with calculations above, the vertically correlated domain state is the stable phase at high temperatures, and the AF coupled phase is metastable. Upon increasing the temperature, thermal fluctuations are sufficient to induce a transition into the vertically correlated remanent state. It is interesting to note that without a magnetic field the vertically correlated domain state is stable down to 40 K, whereas under field cycling, the laterally correlated state begins to emerge at much higher temperatures, as shown in Fig. 1. This confirms a reversal transition dominated by the nucleation mechanism, as found earlier in Ref. 32, Fig. 28.

IV. CONCLUSION

We report on the temperature dependence of the magnetization reversal in $[(Co/Pt)_{X-1}/Co/Ru]_N$ AF coupled multilayer system with $N=3$ and $X=10$. Utilizing the FORC technique, a detailed description of the reversal behavior was obtained. At high temperatures, the AF interlayer coupling is overcome by the dipolar fields, resulting in the nucleation of vertically correlated reverse domains throughout the entire film thickness. The reversal behavior is comparable to a Co/Pt multilayer with no AF coupling of identical thickness. At lower temperatures, the reversal becomes bimodal and results in feature-rich FORC distributions with distinct Co/Pt-like patterns. For example, at 200 K, the middle Co/Pt stack reverses first in a laterally correlated fashion; then, the outer two layers reverse together, in a vertically correlated fashion, and drive part of the reverse domains back into the middle stack, thus triggering a transition into the FM stripe domain reversal mode. Magnetic field cycling leads to exotic reversal behavior where portions of the FORC's extrude outside of the major hysteresis loop, as a result of the conversion between the two modes. Energy calculations show that the laterally correlated remanent state is slightly more stable than the vertically correlated one at lower temperatures. The energy difference diminishes with increasing temperature, largely due to the reduction in the AF interlayer exchange coupling, and eventually the vertically correlated reversal dominates at higher temperatures. The transition in the reversal behavior during an external field sweep is initiated by the dipolar fields from the partially reversed outer stacks.

ACKNOWLEDGMENTS

We thank Randy K. Dumas for technical help. Work at UCD has been supported in part by ACS (PRF-43637-AC10) and the Alfred P. Sloan Foundation (K.L.). J.E.D. acknowledges partial support from NRC.

*Author to whom correspondence should be addressed: kailiu@ucdavis.edu

[1] C. Kooy and U. Enz, Philips Res. Rep. **15**, 7 (1960).
[2] P. F. Carcia, A. D. Meinhaldt, and A. Suna, Appl. Phys. Lett. **47**, 178 (1985).
[3] B. N. Engel, C. D. England, R. A. Vanleeuwen, M. H. Wiedmann, and C. M. Falco, J. Appl. Phys. **70**, 5873 (1991).
[4] C. Chappert, H. Bernas, J. Ferre, V. Kottler, J. P. Jamet, Y. Chen, E. Cambril, T. Devolder, F. Rousseaux, V. Mathet, and H. Launois, Science **280**, 1919 (1998).
[5] O. Hellwig, S. Maat, J. B. Kortright, and E. E. Fullerton, Phys. Rev. B **65**, 144418 (2002).
[6] O. Hellwig, A. Berger, and E. E. Fullerton, Phys. Rev. Lett. **91**, 197203 (2003).
[7] J. E. Davies, O. Hellwig, E. E. Fullerton, G. Denbeaux, J. B. Kortright, and K. Liu, Phys. Rev. B **70**, 224434 (2004).
[8] Z. Y. Liu, L. P. Yue, D. J. Keavney, and S. Adenwalla, Phys. Rev. B **70**, 224423 (2004).
[9] M. S. Pierce, C. R. Buechler, L. B. Sorensen, J. J. Turner, S. D. Kevan, E. A. Jagla, J. M. Deutsch, T. Mai, O. Narayan, J. E. Davies, K. Liu, J. H. Dunn, K. M. Chesnel, J. B. Kortright, O. Hellwig, and E. E. Fullerton, Phys. Rev. Lett. **94**, 017202 (2005).
[10] T. Thomson, G. Hu, and B. D. Terris, Phys. Rev. Lett. **96**, 257204 (2006).
[11] B. Rodmacq, V. Baltz, and B. Dieny, Phys. Rev. B **73**, 092405

(2006).
[12] C. J. Kinane, A. K. Suszka, C. H. Marrows, B. J. Hickey, D. A. Arena, J. Dvorak, T. R. Charlton, and S. Langridge, Appl. Phys. Lett. **89**, 092507 (2006).
[13] A. Baruth, L. Yuan, J. D. Burton, K. Janicka, E. Y. Tsymbal, S. H. Liou, and S. Adenwalla, Appl. Phys. Lett. **89**, 202502 (2006).
[14] Y. L. Iunin, Y. P. Kabanov, V. I. Nikitenko, X. M. Cheng, D. Clarke, O. A. Tretiakov, O. Tchernyshyov, A. J. Shapiro, R. D. Shull, and C. L. Chien, Phys. Rev. Lett. **98**, 117204 (2007).
[15] J. Sort, B. Rodmacq, S. Auffret, and B. Dieny, Appl. Phys. Lett. **83**, 1800 (2003).
[16] P. Grünberg, R. Schreiber, Y. Pang, M. B. Brodsky, and H. Sowers, Phys. Rev. Lett. **57**, 2442 (1986).
[17] S. S. P. Parkin, N. More, and K. P. Roche, Phys. Rev. Lett. **64**, 2304 (1990).
[18] O. Hellwig, T. L. Kirk, J. B. Kortright, A. Berger, and E. E. Fullerton, Nat. Mater. **2**, 112 (2003).
[19] O. Hellwig, A. Berger, and E. E. Fullerton, J. Magn. Magn. Mater. **290-291**, 1 (2005).
[20] O. Hellwig, A. Berger, and E. E. Fullerton, Phys. Rev. B **75**, 134416 (2007).
[21] Y. Fu, W. Pei, J. Yuan, T. Wang, T. Hasegawa, T. Washiya, H. Saito, and S. Ishio, Appl. Phys. Lett. **91**, 152505 (2007).
[22] J. Sort, B. Rodmacq, F. Garcia, S. Auffret, and B. Dieny, J. Appl. Phys. **95**, 7163 (2004).
[23] C. R. Pike, A. P. Roberts, and K. L. Verosub, J. Appl. Phys. **85**, 6660 (1999).
[24] H. G. Katzgraber, F. Pazmandi, C. R. Pike, K. Liu, R. T. Scalettar, K. L. Verosub, and G. T. Zimanyi, Phys. Rev. Lett. **89**, 257202 (2002).
[25] J. E. Davies, O. Hellwig, E. E. Fullerton, J. S. Jiang, S. D. Bader, G. T. Zimanyi, and K. Liu, Appl. Phys. Lett. **86**, 262503 (2005).
[26] S. Maat, K. Takano, S. S. P. Parkin, and E. E. Fullerton, Phys. Rev. Lett. **87**, 087202 (2001).
[27] J. E. Davies, J. Wu, C. Leighton, and K. Liu, Phys. Rev. B **72**, 134419 (2005).
[28] F. Preisach, Z. Phys. **94**, 227 (1935).
[29] I. D. Mayergoyz and G. Friedmann, IEEE Trans. Magn. **24**, 212 (1988).
[30] R. K. Dumas, C. P. Li, I. V. Roshchin, I. K. Schuller, and K. Liu, Phys. Rev. B **75**, 134405 (2007).
[31] J. Olamit, K. Liu, Z. P. Li, and I. K. Schuller, Appl. Phys. Lett. **90**, 032510 (2007).
[32] O. Hellwig, A. Berger, J. B. Kortright, and E. E. Fullerton, J. Magn. Magn. Mater. **319**, 13 (2007).